

## Numerical simulation and experimental investigation of mass transfer in liquid-liquid jets

A. Mirzazadeh ghanadi <sup>1\*</sup>, A.Heydari nasab <sup>1</sup>, D. Bastani <sup>2</sup>

<sup>1</sup>Department of Chemical Engineering, Science and Research Branch , Islamic Azad University, Tehran, Iran

<sup>2</sup>Department of Chemical and Petroleum Engineering, Sharif University of Technology, Tehran, Iran

Received August 23, 2013; Revised December 19, 2013

This paper covers investigation of nozzle diameter and jet velocity effects on mass transfer coefficient under jetting mode by using experimentation and numerical simulation. For this purpose, a chemical system of n-butanol-succinic acid-water was selected and then vertical liquid jet, containing n-butanol and succinic acid, was injected from nozzles (with inside diameters of 1, 2, and 5 mm) into continuous liquid phase (water) axisymmetrically. The level set method was applied for numerical simulation of mass transfer between the liquid jet and the continuous liquid. It was revealed that the results obtained from numerical simulation are in good agreement with experimental data and the mean overall mass transfer coefficient for jet mode is on the scale of  $10^{-3}$  m/s. Also the results of both experimental data and numerical simulation indicate that the overall mass transfer coefficient of the jetting mode is almost one hundred times greater than that of the dropping mode.

**Key words:** liquid- liquid extraction; jetting mode; mass transfer; numerical simulation.

### INTRODUCTION

Many industrial chemical processes include multiphase flows (e.g. multiphase flow reactors, liquid-liquid extraction, etc) that can be categorized as liquid-solid, gas-liquid and liquid-liquid flows. From fluid mechanics aspects, multiphase flows can be taken into account in a mixture in the separated phase from at some scales quite above the molecular level [1]. By moving from one phase to other ones, interfaces and physical properties changes and a complicated behavior is seen near the interface that has not been observed in the single phases.

In a liquid-liquid extraction system it is assumed that a liquid jet is injected into an immiscible liquid phase without any reaction. When a liquid jet is injected with a low velocity from an orifice into a stationary continuous liquid phase, droplets are formed on the outlet of the orifice and no jet is observed. By increasing the velocity at drops change to jet whose length becomes greater with increasing the velocity. When the velocity reaches a maximum, the jet axisymmetric form becomes unstable and the jet begins to break up. Kitamura and Takahashi [2] studied the length of the jet as a function of velocity and various observations of the breakup modes.

It is noteworthy to say that in multiphase flows, before solving the mass transfer equations, interface problem should be solved. There are various methods in literature for solving the convection-diffusion equations under multiphase flows condition. Kim *et al.* [3] studied on phase-field model for breaking up liquid-liquid jet in comparison with experimental data. Numerical simulation on an axisymmetric jet in liquid-liquid systems was studied by Richards *et al.* [4-6], using volume of fluid method. Homma *et al.* [7] utilized direct numerical simulation for solving the Navier Stokes equations by using the front-tracking method. In all aforementioned works the formation of a liquid jet and its break up into droplets in another immiscible liquid were considered. Most of the researches conducted on mass transfer in two-phase flow focus on the droplets and fewer works were done with respect to the jetting mode. Mass transfer across a moving droplet was simulated by adopting a two stage approach (Deshpande and Zimmerman [8]) which decouples the convection-diffusion equations from the governing equations at the level set method. Mass transfer coefficients obtained from simulations are found to be in the same order of magnitude as those obtained by using empirical correlations. Front-tracking method for computations of interfacial flows with soluble surfactants was studied by Muradoglu and Tryggvason [9]. They studied the axisymmetrical motion and deformation of a moving viscous drop

\* To whom all correspondence should be sent:  
E-mail: asgharmirzazadeh@yahoo.com

in a circular tube. Also Marangoni effect with mass transfer in single drops (Wang *et al.* [10]) and during drops formation (Wang *et al.* [11]) were simulated in liquid–liquid extraction by level set method. Hysing [12] developed mixed element FEM level set method for numerical simulation of a rising bubble in an immiscible fluid and then compared the results of simulation with those of some commercial softwares. Using the level set method, mass transfer during drops formation was studied by Lu *et al.* [13] for a chemical system of MIBK–acetic acid–water and good agreement between experimental and simulation results was observed. It is clear that all the mentioned methods have some advantages and disadvantages that make them appropriated or unsuitable for solving various types of problems. For example, in the volume of fluid method since the interface is represented in terms of volume fraction, it is necessary to consider mass conservation issues. For this, reconstruction algorithm is used that causes the numerical solution more complicated. Also in the front-tracking method, rigridding algorithm is employed which gives more complex computations.

In this paper to investigate the mass transfer in liquid-liquid extraction in the jetting mode without breakup, laboratory experiments were conducted and simultaneously the jet system was simulated by using numerical methods. It should be noted that to give less complicated calculations, the level set method is used in the numerical simulation.

### The governing equations

The level set method (Osher [14], Sethian [15]) is based on a function ( $\varphi$ ) which describes the evolution of the interface between two phases. Motion of the interface is solved by level set function ( $\varphi$ ), represented as equation (1).

$$\varphi_t + u \cdot \nabla \varphi = 0 \quad (1)$$

where  $\varphi_t$  is level set function transformed by the advection equation and  $u$  is the fluid velocity.

Fluid pressure and velocity are obtained by solving the incompressible Navier Stokes and continuity equations as equation (2) and equation (3), respectively.

$$\rho \left( \frac{\partial u}{\partial t} + u \cdot \nabla u \right) - \nabla \cdot \mu (\nabla u + (\nabla u)^T) = -\nabla p + \rho g + \sigma \kappa \delta n \quad (2)$$

$$\nabla \cdot u = 0 \quad (3)$$

Where  $\sigma$  is the surface tension,  $n$  and  $\delta$  are unit normal and Dirac delta function, respectively.  $\kappa$  stands for the local interfacial curvature and expressed as equation (4).

$$\kappa_{(\varphi)} = \nabla \cdot n = -\nabla \cdot \left( \frac{\nabla \varphi}{|\nabla \varphi|} \right) \quad (4)$$

$$|\nabla \varphi| = \sqrt{\left( \frac{\partial \varphi}{\partial x} \right)^2 + \left( \frac{\partial \varphi}{\partial y} \right)^2} \quad (5)$$

Fluid density,  $\rho$ , and viscosity,  $\mu$ , can be defined by using Heaviside function as follows :

$$\rho_{(\varphi)} = \rho_{(c)} H_{(\varphi)} + \rho_{(d)} (1 - H_{(\varphi)}) \quad (6)$$

$$\mu_{(\varphi)} = \mu_{(c)} H_{(\varphi)} + \mu_{(d)} (1 - H_{(\varphi)}) \quad (7)$$

$H$  is Heaviside function, a smoothed function written in different ways, expressed by Sussman *et al.* [16, 17] as equation (8).

$$H_{(\varphi)} = \begin{cases} 0 & \text{if } \varphi < -\varepsilon \\ \frac{1}{2} & \text{if } |\varphi| = \varepsilon \\ 1 & \text{if } \varphi > \varepsilon \end{cases} \quad (8)$$

where  $\varepsilon$  is the thickness of interface.

Mass transfer from dispersed phase to continuous one, including convection and diffusion, can be expressed as equation (9).

$$\frac{\partial C_A}{\partial t} + u \cdot C_A = D_A \nabla^2 C_A \quad (9)$$

where  $C_A$  and  $D_A$  are concentration and diffusion coefficient of species A, respectively.  $D_A$  can be obtained as:

$$D_{A(\varphi)} = D_{Ac(\varphi)} + D_{Ad(\varphi)} (1 - H_{(\varphi)}) \quad (10)$$

where  $D_{Ac}$  and  $D_{Ad}$  are the solute diffusion coefficients in the continuous and dispersed phases, respectively.

### EXPERIMENTAL SECTION

The experimental apparatus shown in Figure 1 consists of the following parts: (1) a cylindrical vessel with 10 cm inside diameter and 50 cm height. (2) three glass nozzles with 1, 2 and 5 mm inside diameters. (3) syringe pump with adjustable flow rate. (4) syringe with the volume of 50 cc.

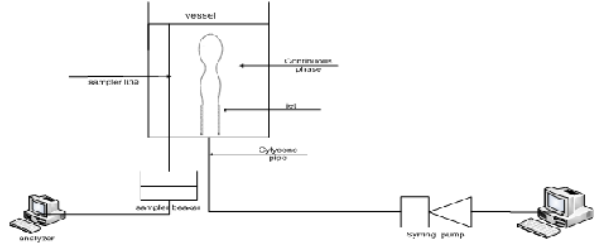


**Fig 1.** Scheme of experimental apparatus

The chemical system was chosen according to standard test system, recommended by EFCE, which contains succinic acid (99%), deionized

**Table 1.** Physical properties of continuous phase and dispersed phase

$\rho_c$ (kg/m <sup>3</sup> )	$\rho_d$ (kg/m <sup>3</sup> )	$\mu_c$ (kg/m.s)	$\mu_d$ (kg/m.s)	$\sigma$ (N/m)	$D_c$ (m <sup>2</sup> /s)	$D_d$ (m <sup>2</sup> /s)
989	852	0.00146	0.0034	1.3x10 <sup>-10</sup>	5.2x10 <sup>-10</sup>	2.1x10 <sup>-10</sup>

water and *n*-butanol (99%). Prior to the experimentation, deionized water and *n*-butanol were saturated by each other to prevent the effect of partial solution on the mass transfer. The amount of succinic acid transferred from the organic phase into the aqueous phase was analyzed by titration using 0.1N sodium hydroxide in the presence of phenolphthalein indicator, while the concentration of succinic acid in inlet was kept 1 wt%. It should be noted that all chemicals used in the experiments are laboratory grade produced by Merck. The physical properties of the system are obtained as below and listed in Table 1.

1-Densities of the saturated aqueous and organic solution were measured by a picnometer in 20 °C.

2- Viscosities of the saturated aqueous and organic solution were measured by an Ostwald viscometer in 20 °C.

3-Interfacial tension and diffusivity coefficients of succinic acid in aqueous and organic phases are provided by EFCE.

According to EFCE, distribution coefficient of solute (succinic acid) between aqueous and organic phases is approximately considered as 1. The height of continuous phase in vessel should be kept at approximately 4 cm, in which the injected jet neither break nor drop.

## RESULTS AND DISCUSSION

### Numerical simulation

A jet with initial velocity,  $u$ , surrounded by an incompressible Newtonian fluid is considered and the velocity is adjusted to prevent jet breaking. Mean overall mass transfer coefficient,  $k_{moA,com}$ , between disperse and continuous phases is computed as equation (11).

$$k_{moA,com} = \frac{\overline{N}_A}{\overline{C}_{A,d} - \overline{C}_{A,c}} \quad (11)$$

where  $\overline{C}_{A,c}$  and  $\overline{C}_{A,d}$  are average concentrations of succinic acid in continuous (water) and disperse (*n*-butanol) phases, respectively defined as:

$$\overline{C}_{A,c} = \frac{\iiint_{\varphi>0.1} C_A dV}{\iiint_{\varphi>0.1} dV} \quad (12)$$

$$\overline{C}_{A,d} = \frac{\iiint_{\varphi<0.1} C_A dV}{\iiint_{\varphi<0.1} dV} \quad (13)$$

$$\mathbf{N}_A = \mathbf{J} = -n \cdot D_A \nabla C_A \quad (14)$$

$\mathbf{N}_A$  is total mass flux at the interface that can be equal with diffusive flux( $\mathbf{J}$ ).

$$\overline{N}_{A,\varphi=0.1} = \frac{\iint_{\varphi=0.1} N_A dA}{\iint_{\varphi=0.1} dA} \quad (15)$$

$\overline{N}_A$  is average flux on surface area at a place where level set function is equal to one tenth ( $\varphi = 0.1$ ).

In this work, these assumptions for numerical modeling of the jet system were applied:

1- Jet velocity and pressure are kept constant.

2- Jet form is axisymmetric which leads to a constant interfacial area.

3- Concentration has no effect on surface tension.

4- Viscosities and densities are constant.

The numerical simulation was conducted by using finite element method in COMSOL software. For this purpose, five steps were taken. in the first step, the vessel with nozzle was drawn by a rectangular in 2D to consider the jet axial symmetric motion in the vessel. In the second step, the object was meshed by using triangle meshes. Equations and boundary conditions were set in the third step. In the fourth step the simulation was run with time step 0.01s and the solution method of BDF (backward differentiation formula). Finally, concentration and flux profiles were studied for each nozzle.

Mesh size influences were investigated for a nozzle with 1 mm inside diameter and it was shown (Figure 2) that beyond the mesh number of 4000, the mean overall mass transfer coefficient reaches the smooth mode, so no more increase in mesh number is needed.

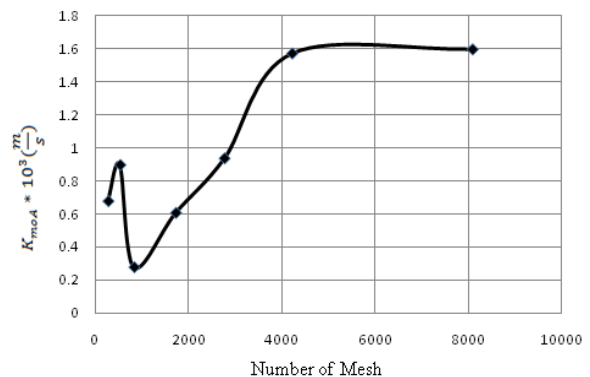


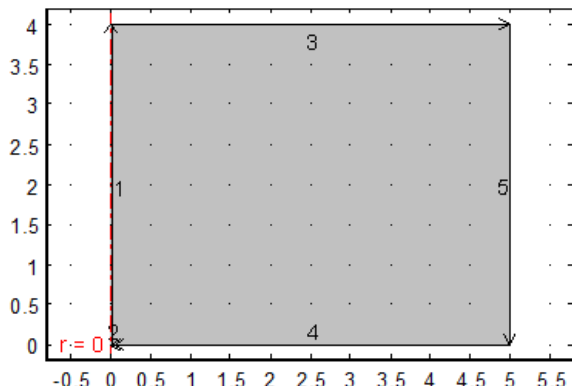
**Fig 2.** Independence test: mean overall mass transfer coefficient versus mesh grid.



**Table 2.** Kinds of boundary conditions with boundary equations

Boundary conditions	Kind of the boundaries	momentum	mass
1	Axial symmetry	Axial symmetry	Axial symmetry
2	inlet	$u = u_0 n$	$C_{A,i} = C_{A,o}$
3	open	$[-pI + \mu(\nabla u + (\nabla u)^T)]n = 0$	$-n \cdot D_A \nabla C_A = 0$
4,5	wall	$u = 0$	$-n N_A = 0$

Boundary conditions are shown in the schematics in Figure 3. Two groups of boundary conditions were applied; the first one is related to momentum transfer and the other one is in connection with mass transfer. Table 2 demonstrates employed boundary conditions in this system.


**Fig 3.** Boundary conditions for system

#### Experimental results

The mean overall mass transfer coefficient is defined by the following equation

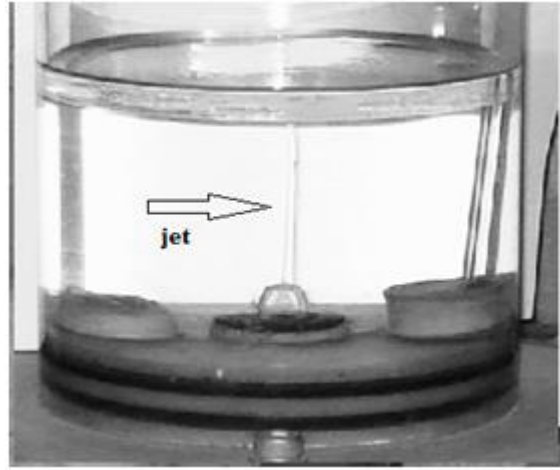
$$R = Q_A (C_{A,i} - C_{A,o}) = k_{moA} S \Delta C_m \quad (16)$$

where  $R$  is mean concentration driving force that usually is a logarithmic average.

$$\Delta C_m = \frac{(C_{A,i} - C_{A,i}^*) - (C_{A,o} - C_{A,o}^*)}{\ln \left[ \frac{(C_{A,i} - C_{A,i}^*)}{(C_{A,o} - C_{A,o}^*)} \right]} \quad (17)$$

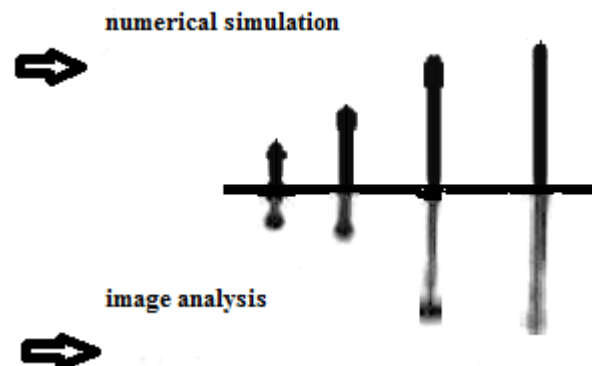
$C_{A,i}^*$  and  $C_{A,o}^*$  are the concentrations in equilibrium with continuous phase in the inlet and the outlet, respectively. Since the continuous phase volume is bigger than that of dispersed phase, external resistance becomes negligible compared to internal one.

In equation 14  $R$ ,  $Q_A$ ,  $S$  are the extraction rate, the volumetric flow rate of disperse phase, and the mass transfer surface area, respectively. As shown in Figure 4 the experiments were conducted under jetting mode without any breakup.


**Fig 4.** Jetting mode for experimental condition

#### Comparison between experimental data and numerical simulation results

Figure 5 depicts a comparison between the shapes resulted from numerical simulation and those obtained from experiments. In Figure 5 the image shown in bottom demonstrates the picture of the jet in real size, taken by a high speed camera, and the one shown at the top depicts the results of numerical calculations. As it can be seen in Figure 5 there is a good agreement between numerical simulation and experimental data.


**Fig 5.** Comparison between numerical simulation results and real picture of the jet.

The experimental and numerical analysis for the effect of nozzle inside diameter in various velocities is shown in Figure 6. It can be observed in Figure 6, mean overall mass transfer coefficient

enhances with increasing jet velocity, whereas it decreases with increasing nozzle diameter.

As shown in Figure 6 the mean overall mass transfer coefficient for jet mode is in the scale of while this quantity for a nozzle with the same diameter size is calculated in the scale of for dropping mode [18, 19]. This enhancement in overall mass transfer coefficient from dropping mode to jetting one can be explained by penetration theory. In this theory the overall mass transfer coefficient is inversely proportional to the exposed time, so by increasing the velocity of the dispersed phase, which leads to the reducing of the exposed time, the overall mass transfer coefficient enhances. Also it can be seen in Figure 6 that with increasing the nozzle diameter the mean overall mass transfer coefficient decreases. This observation can be attributed to the fact that in cylindrical systems when the characteristics length increases, the mass transfer coefficient decreases expressed as follows:

$$Sh = C Re^m Sc^n, \quad m < 1 \quad (18)$$

Also it can be found from Fig. 6 that the maximum deviation between numerical simulation and experimental results for  $k_{moA}$  is  $\pm 10\%$ , indicating good agreement between calculated results and numerical data.

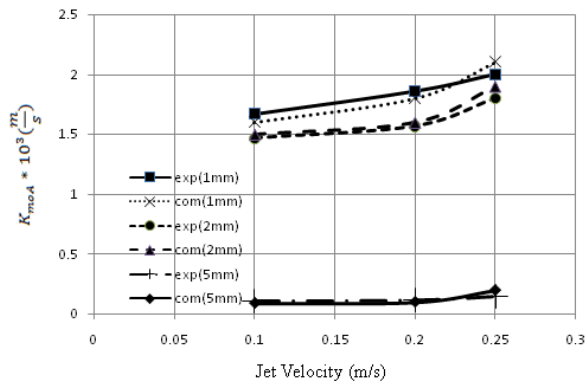


**Fig 6.** Comparison between experimental data and numerical simulation

## CONCLUSIONS

A level set method is used for numerical simulation of mass transfer from a stable jet which moves in a continuous immiscible liquid without any break up. At constant velocity and continuous phase height, with increasing the

nozzle diameter the mass transfer coefficient decreases. When no mode change occurs, with increasing the dispersed phase velocity, the mass transfer coefficient increases at constant height and nozzle diameter. By changing the mode from dropping to jetting, mass transfer coefficient increases with increasing the dispersed phase velocity at constant height and nozzle diameter.

## REFERENCES

1. G. H. Yeoh, J. Tu. Computational Techniques for Multi-phase Flows .Inst.Chem.Eng, 2010.
2. Y. Kitamura, T. Takahashi. Encyclopedia. fluid mechanics, vol.2Gulf, Houston.1986.
3. C. H. Kim, S. H. Shin, H.G. Lee , J .Kim. J. Korean Physical. Society, 55,4 ( 2009) 1451-1460.
- 4.J.R. Richards, A.N. Beris, A.M. Lenhoff, . Phys. Fluids. A ,5 (1993) 1703–1717.
- 5.J.R Richards,, A.M.Lenhoff, , A.N. Beris,, Phys. Fluids., 6 (1994) 2640–2655.
- 6.J.R. Richards, A.N. Beris, A.M.Lenhoff. Phys.Fluids. 7 (1995) 2617–2630.
- 7.S. Homma, J. Koga, S. Matsumoto, M. Song, G. Tryggvason. Chem. Eng. Sci. 6(2006) 3986-3996.
- 8.K. B. Deshpande, W.B Zimmerman. Chem.Eng. Sci. 61(2006) 6486-6498.
- 9.M. Muradoglu , G. Tryggvason. J. Comp. phys .227 (2008) 2238-2262.
- 10.S. Hysing, J. Com.phys.231 (2012) 2449-2465.
- 11.J.F.Wang, C.Wang, Z.S. Mao.Sci. China. 51 (2008) 684-694.
- 12.Z.Wang, P. Lu, Y. Wang, C. Yang, Z.S. Mao. AICH.59 (2013) 4424-4439.
- 13.P.Lung, Z.Wang, C.Yang, Z.S.Mao, Chem. Eng .Sci.65 (2010) 5517-5526.
14. S. Osher, J. A. Sethian. J. Com.phys.79, 1 (1988) 12-49.
15. J. A. Sethian., Cambridge, (1999) p.1-60.
16. M. Sussman, E. Fatemi, P.Smereka, S. Osher. Fluids. Comp. phys. 27 (1998) 663-680.
17. M. Sussman , P.Smereka , S. Osher .J. Com.phys.114 (1994) 146-159.
18. C. Yang, Z,S Mao. Chem. Eng .Sci.60 (2005) 2643- 2660.
19. J. Wang, P. Lu, Z .Wang, C. Yang, Z..S. Mao. Chem. Eng. Sci.63 (2008) 3141 – 3151.

.1

ЧИСЛЕНО СИМУЛИРАНЕ И ЕКСПЕРИМЕНТАЛНО ИЗСЛЕДВАНЕ НА  
МАСОПРЕНАСЯНЕТО В ТЕЧНО-ТЕЧНИ СТРУИ

А. Мирзазадеганади<sup>1\*</sup>, А. Хейдаринасаб<sup>1</sup>, Д. Бастани<sup>2</sup>

<sup>1</sup>Департамент по инженерна химия, Научни-изследвателски клон, Исламски университет «Асад», Техеран,  
Иран

<sup>2</sup>Департамент по инженерна химия и нефтохимия, Технологичен университет “Шариф”, Техеран, Иран

Постъпила на 23 август, 2013 г.; коригирана на 19 декември, 2013 г.

(Резюме)

Работата засяга изследването влиянието на диаметъра на отверстието и скоростта на струята върху коефициента на масопренасяне чрез числено симулиране и експерименти. Използвана е системата n-бутанол–янтарна киселина–вода. Вертикални струи от сместа n-бутанол–янтарна киселина са инжектирани през отверстия с вътрешен диаметър от 1, 2 и 5 mm) във вода като непрекъсната фаза. Установено е, че резултатите от симулирането са в добро съгласие с опитните данни. Осредненият общ коефициент на масопренасяне за струйно течение е около  $10^{-3}$  m/s. Освен това и двете групи резултати показват, че общият коефициент на масопренасяне при струйно течение е почти 100 пъти по-голям, отколкото при капково течение.